Celastrol-based nanomedicines as modulators of neuroinflammation

Sebastien Boridy, Eliza Hutter, Ghareb Soliman, and Dusica Maysinger

Department of Pharmacology and Therapeutics, Faculty of Medicine, McGill University, Montreal, Qc, Canada
sebastien.boridy@mail.mcgill.ca; dusica.maysinger@mcgill.ca

ABSTRACT

Celastrol is a promising anti-inflammatory and antioxidant therapeutic for diseases of the central nervous system involving chronic activaton of microglia, the main innate immune effector cells of the brain. However, celastrol exhibits low aqueus solubility and a narrow therapeutic index. Herein, we propose the use of nanodelivery systems (e.g. neutral and cationic PAMAM dendrimers and gold nanoparticles) for the efficient solubilisation and delivery of celastrol to microglia. We show significant decreases in inflammatory mediator release (e.g. nitric oxide) and inflammatory signaling (i.e. p38 inhibition) in LPS-stimulated microglia. Furthermore, gold nanorods loaded with celastrol localised to mitochondria in microglia, an important sire of action for celastrol. Results from this study suggest the potential of nanodelivery systems for CNS-targeted anti-inflammatory therapies.

Keywords: Poly(amido amine), gold nanoparticles, celastrol, microglia, neuroinflammation

1 BACKGROUND

Chronic inflammation, particularly in neurodegeneration, plays a pivotal role in promoting disease pathology in the central nervous system (CNS). Microglial cells, which represent the main innate immune effector cells in the CNS, orchestrate these neuroinflammatory reactions that ultimately determine whether the response to injury will be protective or destructive. As such, microglia are ideal targets for anti-inflammatory therapies aimed at reducing inflammation in the CNS. Celastrol, a naturally occurring quinone methide triterpene, has long been used in traditional Chinese medicine for the treatment of cancer and inflammatory diseases. Celastrol can upregulate cytoprotective molecular chaperones in neuronal cells [1] and inhibit NFκB-mediated inflammatory signaling [2]. However, its low water solubility and toxicity represent major pitfalls for drug delivery in the clinic. Our group has recently begun investigating nano-delivery systems for celastrol. Dendrimers are of particular interest due to their amphiphilic nature, predictable tree-like architecture, polyvalency, and monodisperse, stable structure [3]. Poly-(amidomine) (PAMAM) dendrimers are the most widely studied dendrimers to date and exhibit inherent anti-inflammatory activity in vivo [4]. Alternatively, gold nanoparticles (GNPs) have also been considered due to their biocompatibility, facile conjugation to biomolecules, tunable size and shape, in addition to their imaging capabilities. Our group has already shown how GNP shape and size can be tailored to regulate microglial function [5].

The overall objective of the present study was to develop a viable approach to deliver celastrol to reactive microglia with the aim of inhibiting neuroinflammatory responses. Our results show that PAMAM dendrimers, alone, and in complexation with celastrol attenuate release of inflammatory mediators and inhibit inflammatory signaling through MAPK in lipopolysaccharide (LPS)-stimulated microglia. Additionally, we provide evidence that gold nanoparticles are potential candidates for the delivery of anti-inflammatory therapies (e.g. celastrol) to CNS-resident microglia in disease states characterized by chronic microglial activation, such as Alzheimer's disease (AD).

2 MATERIALS AND METHODS

2.1 Materials

Poly(amido amine) (PAMAM or G4) dendrimers, griess reagent, sodium nitrite, and 3-(4,5-dimethylthiazol-2-yl)-2,5-diphenyl tetrazolium bromide (MTT) were purchased from Sigma Aldrich (Oakville, ON, Canada). Celastrol was purchased from PI & PI TECHNOLOGIES Inc., (Taihe, Baiyun, Guangzhou 510540, China). p38-α MAPK, phospho-p38 MAPK (Thr180/Tyr182) antibodies were purchased from Cell Signaling Technologies (Danvers, MA, USA). α-actin antibody was purchased from Millipore (Billerica, MA, USA). All cell culture media and other cell culture labeling kits and reagents were purchased from Invitrogen (Burlington, ON, Canada). All other reagents were purchased from Sigma Aldrich Canada (Oakville, ON, Canada), unless stated otherwise.

2.2 Celastrol solubilisation by PAMAM (G4) dendrimers

Solubility studies of celastrol in aqueous G4-OH and G4-NH_2 (Schematic at left). dendrimer solutions were carried out by the phase solubility method of higuchi and connors with minor modifications [6]. Briefly, pamam stock solutions (25 mg/ml) in PBS (10 mm, ph 7.4) were prepared after completeevaporation of methanol under vacuum at 50 °c and keeping the dried dendrimer films

under nitrogen for 24 h. pH of the pamam solution was readjusted to 7.4 using 0.1 N HCl. An excess of celastrol was added into amber-colored screw-capped

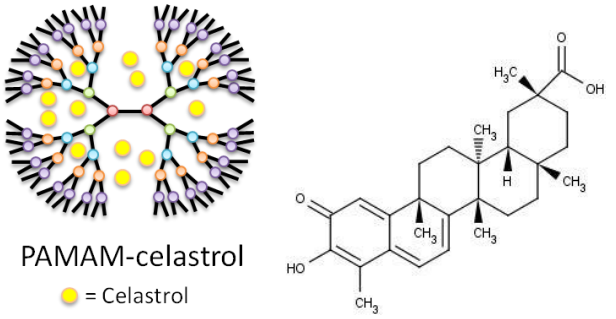

Figure 1. Celastrol complexed with PAMAM dendrimer construct, *at left,* and celastrol structure, *at right.*

glass vials (4 ml) containing varying concentrations (5, 10, 15, 20, 25 mg/ml) of g4-oh and g4-nh$_2$ dendrimers in PBS (pH 7.4). Excess drug was added into a vial containing only PBS (pH 7.4) and was used as control. The mixtures were mechanically shaken at 200 rpm for 24 h followed by centrifugation at 14,000 rpm for 30 min. The supernatant were collected and aliquots were properly diluted with methanol and celastrol concentration was determined by HPLC. The affect of pH on celastrol solubility in an aqueous dendrimer solution (5.0 mg/ml) was studied using dendrimer solutions having pH values preadjusted to 1.2, 3.0, 5.0, 7.4, 9.0 using 0.1 N HCl or 0.1 N NaOH. The mixtures were treated as above and celastrol concentration was determined by HPLC.

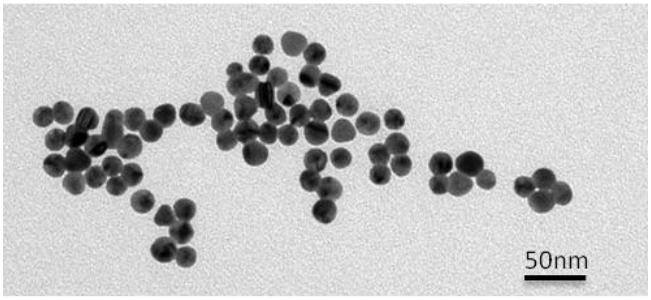

Figure 2. TEM of gold nanoparticle spheres (GNS) loaded with celastrol.

2.3 Preparation of gold nanoparticles.

CTAB-coated spherical GNPs (d = 23.1 ± 1.1 nm) were prepared by adding an aqueous ice-cold $NaBH_4$ solution (0.500 mL, 0.01 M) to a mixture of aqueous $HAuCl_4 \cdot 3H_2O$ (0.125 mL, 0.01 M) and an aqueous solution of CTAB (4.375 mL, 0.075 M). The seed growth was allowed to proceed for 2 h. After this time, an aliquot of the seed solution was added to a solution obtained by adding aqueous CTAB (1.6 mL, 0.10 M), aqueous $HAuCl_4 \cdot 3H_2O$ (2 mL, 0.01 M), an aqueous AA solution (0.6 mL, 0.10 M) to 90 mL water, followed by the aged seed solution (0.1 mL). Immediately upon addition of the seed solution, the mixture was mixed gently for 10 s. It was then kept undisturbed for at least 3 h. The solutions were kept at 27 °C (in a water bath) throughout the entire procedure in order to prevent the crystallization of CTAB. At the end of the reaction, the mixture was centrifuged by an Eppendorf centrifuge model 5403 (6000 rpm, 60 min). The residue was redispersed in water (5 mL). Rod GNPs were synthesized by a scaled-up version of the seeded growth method described previously [7]. CTAB was replaced with PEG following initial formation of rods. CTAB-coated urchin GNPs were also prepared by seed mediated process [8]. Loading of celastrol onto PEGylated gold nanoparticles: The PEGylated gold nanoparticles (0.75 ml) were incubated with celastrol/DMSO (0.015 ml, 10 mM) overnight. To remove excess celastrol, the GNPs were centrifuged (14,000 rpm, 20 minutes) and redispersed in DI water.

2.4 Cell culture and treatments

N9 microglial cells were cultured in Iscove's Modified Dulbecco's Medium (IMDM; Gibco) supplemented with 5% (v/v) fetal bovine serum (FBS; Gibco) and 1% (v/v) penicillin-streptomycin (Gibco). Cells were seeded 24hrs prior to treatment/media change according to the appropriate density for the indicated assay (see below). They were maintained at 37oC with 5% CO2 and >95% relative humidity. Medium was changed to serum free for all treatments, unless indicated otherwise, and lasted for ≤24hrs..

2.5 Measurement of nitric oxide release

Nitric oxide (NO) release was measured using the Griess Reagent (1% sulphanilamide, 0.1% *N*-(1-naphthyl)-ethylenediamine dihydrochloride, 5% phosphoric acid). Sodium nitrite in cell culture media was used to generate a standard curve (0-100uM). After treatment, 50 µL of the supernatant from each well was mixed with 50 µL of Griess reagent in a clear bottom 96-well plate (Sarstedt), and incubated at room temperature for 15 min. Absorbance at 540 nm for each sample was measured in triplicates using the microplate reader.

2.6 Western Blotting

Whole cell extracts were collected, 25 µg were loaded onto a 12% gradient sodium dodecyl sulfate-polyacrylamide gel electrophoresis (SDS-PAGE) and transferred to a nitrocellulose membrane. Membranes were washed with 0.1% Tween-20 + TBS and blocked with 5% milk + 0.5% Tween-20 + TBS for 1 h at room temperature and incubated with rabbit anti-p38, rabbit anti-phospho-

p38, (Cell Signaling Technologies) diluted 1:1000 in blocking solution overnight at 4°C. After five washes with 0.1% Tween-20 + TBS, the membranes were incubated with the HRP conjugated anti-rabbit (Bio-Rad) diluted 1:5000 in 5% milk + 0.5% Tween-20 + TBS for 1 h at room temperature. After five washes with 0.1% Tween-20 + TBS, HRP substrate (Millipore) was added and incubated for 5min, following which the membranes were exposed to film (Harvard). Blotting with mouse anti-actin (Millipore) was used as a housekeeping protein to control for global protein expression levels.

2.7 Two-Photon Luminescence (TPL)

Two-photon imaging was performed on N9 microglia. Images were acquired with a Zeiss LSM 510 upright microscope. A HeNe (633 nm, 0.1% max intensity) in combination with an LP650 filter were used to image MitoTracker Deep Red 633 and a two-photon Ti:sapphire laser (set at 750 nm; 10.0% max intensity) in combination with BP 390-465 IR filter was used to image GNRs. A Plan-Achromat vis−IR 63× NA 1.0 objective was used for all samples. No background fluorescence of cells was detected under the settings used. Images were acquired at a resolution of 1024 × 1024. Images were analyzed using the Zeiss Confocal LSM Image browser, in combination with ImageJ.

2.8 Statistical Analysis

All data were expressed as mean ± sem and analyzed by one-way anova, as indicated. All values were obtained from at least three independent experiments. When a significant effect was obtained with one-way anova, dunnett's test was used to compare all values to the control. Alternatively, student's t-test was used to analyze significant differences between the means of 2-8 groups, and bonferroni's correction was applied where necessary.

3 RESULTS AND DISCUSSION

3.1 Inhibition of nitric oxide (NO) release

It is well recognized that LPS stimulates microglial cells to synthesize and release NO via activation of toll-like receptor 4 (TLR-4) and subsequent upregulation of inducible nitric oxide synthase (iNOS) [9]. To demonstrate the anti-inflammatory activity of celastrol-encapsulated PAMAM dendrimers, microglia were pre-treated as with PAMAM dendrimer constructs or celastrol alone followed by treatment with LPS (10µg/mL) for 24h. Figure 3 clearly shows that G4-NH_2 with and without celastrol was most efficeint at attenuating NO release induced by LPS treatment, however, it simulatneously led to a drastic reduction in cell viability, as determined by the MTT assay. The same is true for celastrol. G4-OH+Cel, on the other hand, drastically reduced NO release in the absence of any observed cytotoxicity.

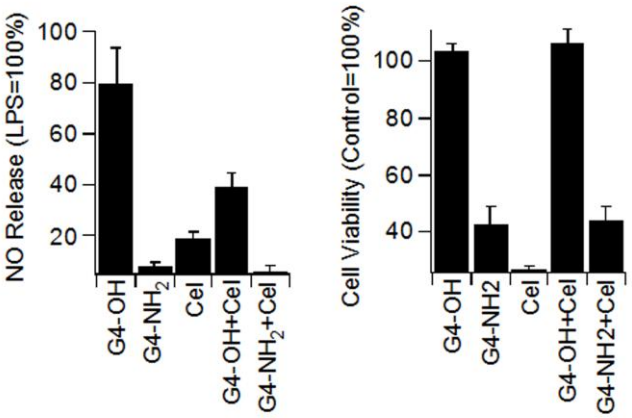

Figure 3. PAMAM-dendrimers inhibit NO release from LPS-stimulated microglia.

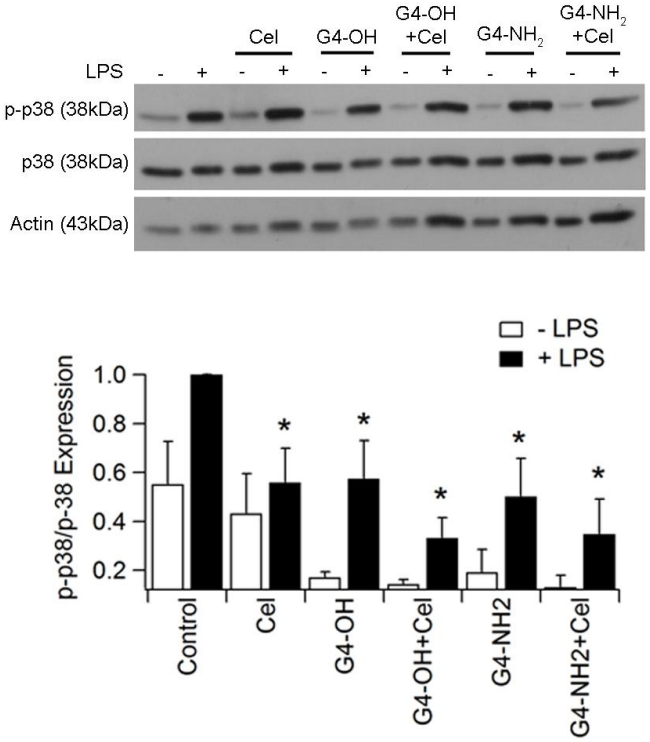

Figure 4. PAMAM-dendrimers inhibit p38 MAPK activation in LPS-stimulated microglia.

3.2 Inhibition of MAPK (p38) activation

The MAPK, p38, is a downstream converging point of the TLR-4 inflammatory signaling cascade and regulates iNOS expression [10]. Given that PAMAM dednrimers diminished NO release, we were looking to investigate how far upstream this inhibitory effect could be traced. Indeed,

we provide evidence supporting an inherent dendrimer-mediated blockade of p38 activation (Figure 4), seen as reduced phoshpho p38 expression (quantification of band intensities in bottom panel) following LPS-stimulation in the presence of G4-OH and G4-NH_2, which is in agreement with the inhibition of NO release (Figure 3). This effect was further enhanced when celastrol was complexed with dendrimers, although no significant ($p>0.05$) difference was found between complexed and uncomplexed dendrimers. This is particularly interesting given the anti-inflammatory activity previously reported for neutral and cationic PAMAM dendrimers via downregulation of COX-2 [4]. Importantly, p38 has been shown to regulate COX-2 expression [11], providing a mechanistic explanation for PAMAM's anti-inflammatory activity.

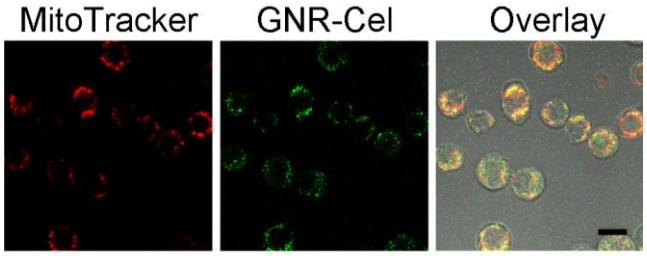

Figure 5. GNR-Cel localizes to mitochondria in microglia cells. Scale bar in image is 10um.

3.3 Mitochondrial targeting

GNPs offer an added advantage over polymeric delivery systems: imaging capabilities. We chose to investigate the delivery and localization of gold nanorods loaded with celastrol (GNR-Cel) to microglial cells. GNPs are known to exhibit a two-photon induced luminescent effect in response to excitation by long wavelength light (~750nm) [12]. GNR-Cel was found to colocalize with mitochondria (Figure 5), which is line with recent reports in cancer cells [13]. Given celastrol's reported antiperoxidation activity in the outer and inner mitochondrial membranes [14], this targeting capability of GNR-Cel may serve a therapeutic purpose in reducing ROS and subsequent activation of inflammatory signaling pathways.

4 CONCLUSION

Herein, we show the capacity of nanodelivery systems to efficeintly load celastrol, exhibit anti-nflammatory activity, and delivery to microglial cells. Specifically, neutral and cationic PAMAM dendrimers were shown to inhibit inflammatory mediator release (e.g. NO) and inflammatory signaling (i.e. p38 inhiition) in LPS-stmulated microglial cells. Moreover, GNR-Cel was shown to localize to mitochondria, the site of action for celastrols antioxidant activity. This study supports the use of nanodelivery systems to improve the therapeutic efficacy of celastrol in disease states of the CNS.

5 ACKNOWLEDGEMENTS

This work was supported by a grant from the Canadian Institutes of Health Research (CIHR). SB is a CIHR Vanier Canada Graduate Scholar.

REFERENCES

1. Chow, A.M. and I.R. Brown, *Induction of heat shock proteins in differentiated human and rodent neurons by celastrol.* Cell Stress Chaperones, 2007. **12**(3): p. 237-44.
2. Zhang, T., et al., *Characterization of celastrol to inhibit hsp90 and cdc37 interaction.* J Biol Chem, 2009. **284**(51): p. 35381-9.
3. Menjoge, A.R., R.M. Kannan, and D.A. Tomalia, *Dendrimer-based drug and imaging conjugates: design considerations for nanomedical applications.* Drug Discov Today, 2010. **15**(5-6): p. 171-85.
4. Chauhan, A.S., et al., *Unexpected in vivo anti-inflammatory activity observed for simple, surface functionalized poly(amidoamine) dendrimers.* Biomacromolecules, 2009. **10**(5): p. 1195-202.
5. Hutter, E., et al., *Microglial response to gold nanoparticles.* ACS Nano, 2010. **4**(5): p. 2595-606.
6. Higuchi, T. and K.A. Connors, *Phase-solubility techniques.* Advances in analytical chemistry and instrumentation, 1965. **4**: p. 117-212.
7. Sau, T.K. and C.J. Murphy, *Seeded high yield synthesis of short Au nanorods in aqueous solution.* Langmuir, 2004. **20**(15): p. 6414-20.
8. Yu, K., et al., *Morphologies and surface plasmon resonance properties of monodisperse bumpy gold nanoparticles.* Langmuir, 2008. **24**(11): p. 5849-54.
9. Matsui, T., et al., *Release of prostaglandin E(2) and nitric oxide from spinal microglia is dependent on activation of p38 mitogen-activated protein kinase.* Anesth Analg, 2010. **111**(2): p. 554-60.
10. Lee, S.Y., et al., *Mitogen activated protein kinases are prime signalling enzymes in nitric oxide production induced by soluble beta-glucan from Sparassis crispa.* Arch Pharm Res, 2010. **33**(11): p. 1753-60.
11. Takai, E., et al., *Involvement of P2Y6 Receptor in p38 MAPK-Mediated COX-2 Expression in Response to UVB Irradiation of Human Keratinocytes.* Radiat Res, 2011. **175**(3): p. 358-66.
12. Zhang, Y., et al., *Gold nanorods for fluorescence lifetime imaging in biology.* J Biomed Opt, 2010. **15**(2): p. 020504.
13. Wang, L., et al., *Selective targeting of gold nanorods at the mitochondria of cancer cells: implications for cancer therapy.* Nano Lett, 2011. **11**(2): p. 772-80.
14. Sassa, H., et al., *Structural basis of potent antiperoxidation activity of the triterpene celastrol in mitochondria: effect of negative membrane surface charge on lipid peroxidation.* Free Radic Biol Med, 1994. **17**(3): p. 201-7.